International Journal of Engineering Science 198 (2024) 104053

Contents lists available at ScienceDirect

International Journal of Engineering Science

journal homepage: www.elsevier.com/locate/ijengsci

Full length article

On nonlinear rheology of masonries and granular media

Emanuele Reccia, Victor A. Eremeyev *

Department of Civil and Environmental Engineering and Architecture (DICAAR), University of Cagliari, Via Marengo, 2, 09123 Cagliari, Italy

ARTICLE INFO

Keywords:
Granular media
Masonry
Cosserat point
Nonlinear rheology

ABSTRACT

We introduce a new rheological nonlinear model for some granular media such as masonries. The latter may demonstrate a rather complex behaviour. In fact, considering a masonry one can see that relative rotations of bricks are most important in comparison with deformation of bricks themselves. As a result, one gets stresses and couple stresses as static characteristics of such a medium. Using the Cosserat point approach for modelling of orientational interactions between masonry elements we provide a deformation energy for such a medium which takes into account both material and geometrical nonlinearity.

1. Introduction

Granular materials constitute a rather challenging object for continuum mechanics. In fact, they may demonstrate both fluid- and solid-like behaviour, see e.g. Capriz et al. (2008), Castellanos (2005), de Gennes (1998, 1999), Hutter and Rajagopal (1994), Kachanov and Sevostianov (2005), Nedderman (1992) and Suiker and de Borst (2005). Moreover, their properties may essentially depend on the interactions between granules. Even in the case of solid-like granular media such as a masonry adhesion/friction/sliding of bricks may be more crucial than their mechanical properties. Considering kinematics of granular media and granules themselves one can see that relative rotations of granules are also essential. So one can expect appearance of couple stresses as a response to rotational degrees of freedom. This observation makes rather natural to exploit the Cosserat continuum model for such a medium.

The aim of this paper is to introduce a nonlinear rheological model for a class of granular media which includes masonries. As a masonry represents a highly inhomogeneous material it is quite natural to use some homogenization techniques for introducing an effective medium, see e.g. Addessi et al. (2013), Anthoine (1995), Bacigalupo and Gambarotta (2012), Cecchi and Sab (2002), Diana et al. (2023), Gatta and Addessi (2023), Lourenço (2010), Luciano and Sacco (1997) and Sacco (2009). Such an approach is particularly suitable for masonry-like materials whose mechanical behaviour is strongly influenced by the internal microstructure. Since the arrangement of the bricks plays a crucial role at the macroscopic level, discrete models – where the constitutive elements of the masonry are modelled separately, see for example Lemos (2007) – may be preferable to properly account for this. At the same time, however, the computational requirements limit their applicability to small parts of buildings, requiring the adoption of more efficient models. Macro-element models – where masonry structures are represented by simplified equivalent structures, such as a system of non-linear beams, see for example Magenes and Calvi (1997) – are usually adopted by practitioners thanks to the possibility of analysing real buildings, but the description of the masonry material is too coarse. In this context, continuum models – where the masonry is modelled as an equivalent continuum able to take into account the internal microstructure, i.e. obtained through homogenization techniques, see the review by Lourenço et al. (1997) – can be an effective solution.

As mentioned by Forest and Sab (1998) instead of having classic Cauchy continuum as an effective medium it could be more efficient to use generalized continua such as Cosserat continuum. This is particularly true in the case of masonry, which may have rotations depending by the interlocking of the bricks. The basic idea of our approach is related to Cosserat-point model by Rubin

* Corresponding author.
E-mail addresses: emanuele.reccia@unica.it (E. Reccia), eremeyev.victor@gmail.com (V.A. Eremeyev).

https://doi.org/10.1016/j.ijengsci.2024.104053
Received 30 December 2023; Received in revised form 1 March 2024; Accepted 2 March 2024
Available online 6 March 2024

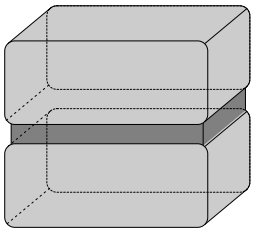

Fig. 1. Two bricks with a mortar layer.

(1985, 2000), see also Jabareen and Pestes (2020) and Jabareen and Rubin (2008) and the references therein, and to nonlinear Cosserat continuum model (Eremeyev et al., 2013; Eringen, 1999), in general. Here we consider both material and geometrical nonlinearities, taking into account finite translations and rotations. In the literature one can find various applications of Cosserat continuum model to granular media and masonries, see e.g. Addessi et al. (2010), Casolo (2006), Colatosti et al. (2023), De Bellis and Addessi (2011), Masiani et al. (1995), Masiani and Trovalusci (1996), Pau and Trovalusci (2012), Reccia et al. (2018), Salerno and De Felice (2009), Stefanou et al. (2008), Tejchman (2008), Thatikonda et al. (2024), Tian et al. (2023), Trovalusci and Masiani (2003) and Trovalusci and Pau (2014), see also the reviews by Baraldi et al. (2015) and D'Altri et al. (2020).

The remainder of the paper is organized as follows. First, in Section 2 we consider experimentally observed behaviour of a such medium. We discuss responses to tension–compression, shear, and relative rotations. For simplicity we assume that our medium consists of rigid bricks with highly deformable (soft) thin interfacial layers. We provide three types of response called "real", "simplified", and "ideal". Then, in Section 3 we use these dependencies to introduce a continuum model. First, we briefly recall basic equations of polar media paying most attention to geometrical sense of strain measures as discussed in Eremeyev et al. (2013), Eringen (1999) and Pietraszkiewicz and Eremeyev (2009). Finally, we present the deformation energy as a sum of energies related to tension-compression, shear, torsion, and bending. Its dependence on masonry ordering, i.e. lattice type, is also discussed.

2. Rheology observations

Masonry is a composite heterogeneous material characterized by an internal microstructure at the mesoscale, consisting of a system of rigid elements – blocks (natural stones, square or rough) or bricks (artificial regular units) – interacting with each other through deformable or non-deformable unilateral interfaces with no or very low tensile strength and resistant to sliding by friction. Masonry makes up a large proportion of the world's existing buildings: much of the historical architectural heritage consists of monumental masonry structures, and in many countries ordinary residential buildings are typically constructed of masonry. Its mechanical behaviour is interesting because it exhibits a highly non-linear behaviour, even for loads far from collapse, and very different responses to compression and tension, with a usually high compressive strength coupled with a very low or uncertain tensile strength, so that it is often considered to be a non-tensile material (Angelillo, 1993; Del Piero, 1989, 1998; Heyman, 1966). Moreover, this complex behaviour is strongly influenced by the constructive characteristics of the masonry: the quality of the constituent materials, the size of the bricks, the thickness of the joints, the arrangement of the bricks, the bonds, etc. The typological diversity, composite nature, heterogeneity and anisotropy of masonry make it difficult to describe its mechanical behaviour.

Experimental studies of masonries were provided in a series of works, see e.g. Baraldi et al. (2021), Dhanasekar et al. (1985), Lourenço et al. (1998), Page (1981) and Vasconcelos and Lourenço (2009a, 2009b). For example, Page (1981) presented non-trivial limit surface under biaxial tension–compression. In particular, Cosserat's effects, such as the orthotropic shear behaviour of brick masonry, were tested recently by Thatikonda et al. (2024).

Here we focus on a simple example of masonry consisting of two bricks connected by an intermediate joint, as shown in Fig. 1. The bricks are assumed to be rigid, while the joint is highly deformable. The following describes the physics of the interaction in terms of compressive-tensile, shear and moment stresses. In particular, the different responses to compression and tension, sliding in relation to shear and relative rotations between the bricks due to moment are highlighted. Both "real", "simplified" and "ideal" behaviour are considered.

2.1. Tension–compression

A typical loading curve for tension-compression test is given in Fig. 2 (curve I). Here σ and ε are engineering stress and engineering strain, respectively. One can see that the mortar material response is not symmetric with respect to tension and compression. Moreover, the material has very low strength under tension. As a result, a simplified linear version can be used as presented in Fig. 2 (curve II). Here σ^* and ε^* are maximal tensile stress and strain, respectively. The corresponding strain energy can be defined through the standard formula

$$W_{TC} = \int \sigma \, d\varepsilon. \tag{1}$$

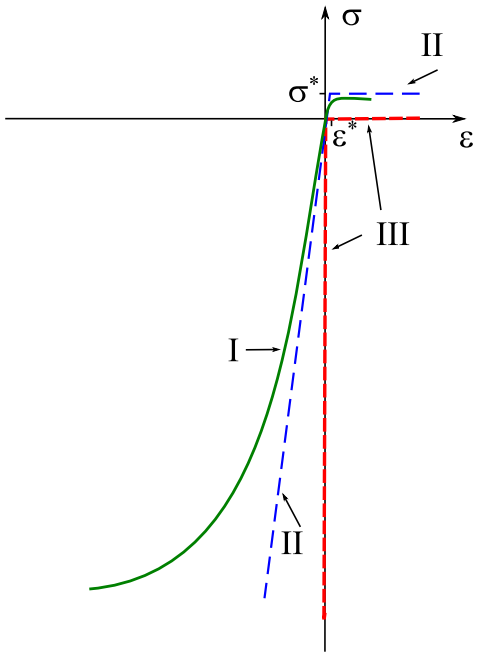

Fig. 2. Tension-compression loading curves. Curves I, II, and III correspond to real, linear simplified, and ideal models.

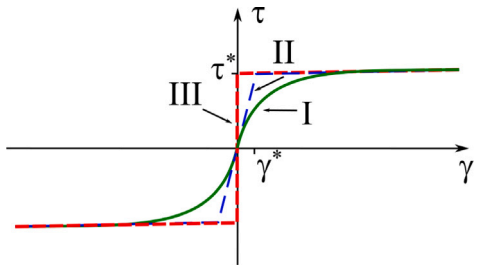

Fig. 3. Loading curves for shear. Curves I, II, and III correspond to real, linear simplified, and ideal models.

In particular, for dependence II it could be calculated as follows

$$W_{TC}^{II} = \begin{cases} \frac{1}{2}E\varepsilon^2, & \varepsilon < \varepsilon^* \\ \sigma^*\varepsilon, & \varepsilon > \varepsilon^* \end{cases}, \tag{2}$$

where E is the Young modulus. Let us note that in the case of simplified version of constitutive equations we may face an issue related to nonexistence of derivative at $\varepsilon = \varepsilon^*$.

As an essential simplification of such a behaviour the non-tension model can be also used, see curve III in Fig. 2. Here material has no tensile strength and become rigid under compression (has unlimited strength under compression). Formally, this case corresponds to $E = \infty$ and $\sigma^* = 0$.

2.2. Shear and sliding

Similar but symmetric behaviour can be observed for shear (sliding), see Fig. 3, where again we present three models (curves I, II, III). Here τ and γ are tangent stress and shear strain, respectively, with ultimate values τ^* and γ^*. The strain energy is defined by the formula

$$W_{Sh} = \int \tau \, d\gamma, \tag{3}$$

that results in the case of simplified model (curve II) in the equation

$$W_{Sh}^{II} = \begin{cases} \frac{1}{2}\mu\gamma^2, & |\gamma| < \gamma^* \\ \tau^*\gamma, & |\gamma| > \gamma^* \end{cases}, \tag{4}$$

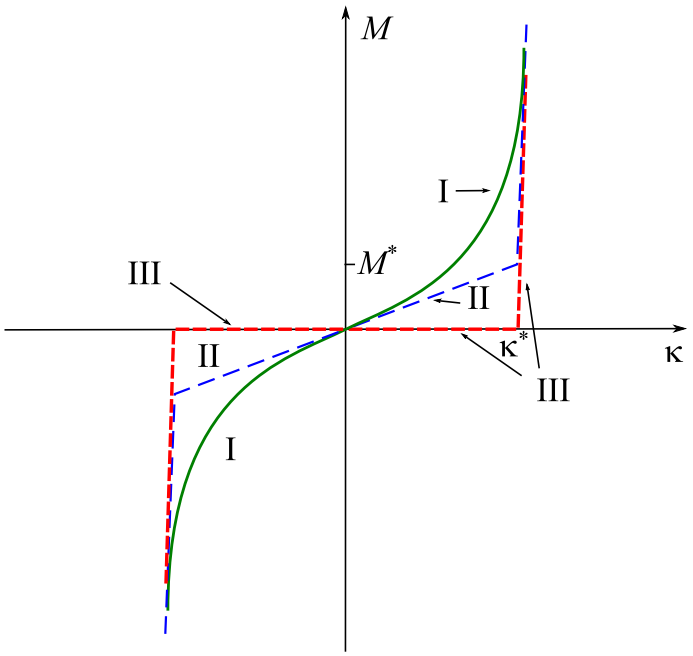

Fig. 4. Moment — relative rotation. Curves I, II, and III correspond to real, linear simplified, and ideal models.

where μ is a shear modulus.

The ideal model III corresponds to the Coulomb friction law.

2.3. Bending

Considering relative rotations of two bricks we can also introduce three models, see Fig. 4. As in the case of tension-compression and shear here we face also with limiting behaviour. Here M and κ are the moment and relative rotation, respectively. Due to geometrical constraints κ has also a limit value κ^* whereas M^* corresponds to maximal admissible moment in an elastic regime.

In the case of linear model (curve II) the general formula for the strain energy

$$W_B = \int M \, d\kappa, \tag{5}$$

results in

$$W_B^{II} = \begin{cases} \frac{1}{2} K \kappa^2, & |\kappa| < \kappa^* \\ \infty, & |\kappa| = \kappa^* \end{cases}, \tag{6}$$

where K is a bending stiffness.

The ideal model (curve III) is similar to rigid-plastic solids but with respect to rotations. It is interesting to note that this constitutive relation is similar to strain-limiting elasticity by Rajagopal (2011). Indeed, unlike the previous cases where we face stress-limiting constitutive relations, in the latter case one see limiting rotations.

2.4. Torsion

The case of torsion is similar to shear presented above. Here we again may provide three models with limiting torsional moment $M*_t$ and torsion κ_t^*. Related to curve II the linear model corresponds to the following strain energy

$$W_T = \int M_t \, d\kappa_t \tag{7}$$

with

$$W_T^{II} = \begin{cases} \frac{1}{2} K_t \kappa_t^2, & |\kappa| < \kappa^* \\ M_t^* \kappa_t, & |\kappa| \geq \kappa_t^* \end{cases}, \tag{8}$$

where K_t is a torsional stiffness (see Fig. 5).

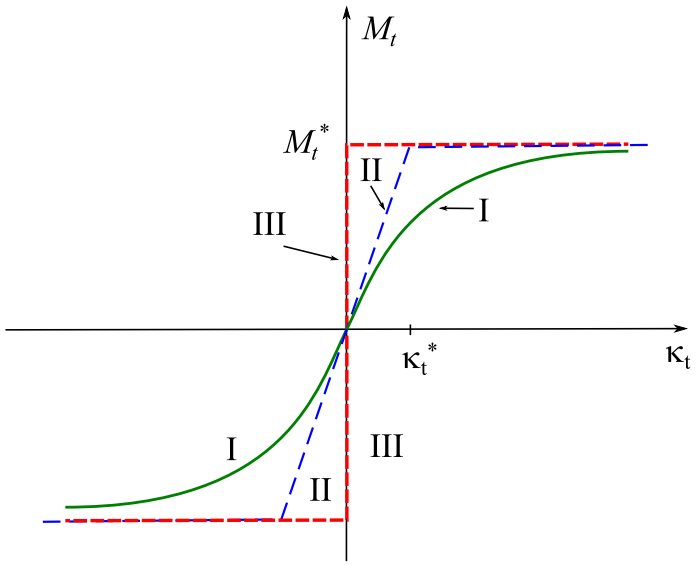

Fig. 5. Torsional moment — relative rotation. Curves I, II, and III correspond to real, linear simplified, and ideal models.

3. Continuum model

In the following, using the previous observations, we discuss the relevant continuum model.

3.1. Micropolar finite elasticity

First, let us briefly recall the basic equations of the Cosserat continuum in the case of finite deformations. The kinematics of Cosserat continuum can be described using two descriptors, i.e. translations and rotations (Eremeyev et al., 2013; Eringen, 1999; Pietraszkiewicz & Eremeyev, 2009)

$$\mathbf{x} = \mathbf{X} + \mathbf{u}(\mathbf{X}, t), \quad \mathbf{Q} = \mathbf{Q}(\mathbf{X}, t), \tag{9}$$

where $\mathbf{x}$ and $\mathbf{X}$ are the position vectors defined in current and reference placements, respectively, t is time, $\mathbf{u}$ is the vector of translations, and $\mathbf{Q}$ is the orthogonal tensor of microrotations.

For hyperelastic materials there exists a deformation energy W introduced as a function of two Lagrangian strain measures

$$W = W(\mathbf{E}, \mathbf{K}), \tag{10}$$

where

$$\mathbf{E} = \mathbf{Q}^T \cdot \mathbf{F}, \quad \mathbf{K} = -\frac{1}{2}\epsilon : (\mathbf{Q}^T \cdot Grad\, \mathbf{Q}). \tag{11}$$

In (11) $\mathbf{F} = Grad\, \mathbf{x}$ is the deformation gradient, $Grad$ is the Lagrangian gradient operator, $\epsilon = -\mathbf{I} \times \mathbf{I}$ is the permutation tensor, $\mathbf{I}$ is the 3D unit tensor, $\cdot$, $:$, and $\times$ stand for the dot, double dot, and cross products, respectively.

Corresponding stress tensors are given by

$$\mathbf{P} = \mathbf{Q} \cdot \frac{\partial W}{\partial \mathbf{E}}, \quad \mathbf{S} = \mathbf{Q} \cdot \frac{\partial W}{\partial \mathbf{K}}. \tag{12}$$

Here $\mathbf{P}$ and $\mathbf{S}$ are the first kind Piola–Kirchhoff stress and couple stress tensors, respectively. Determination of W constitute a rather complex problem, so in the following we specify it using experimental observations of the previous sections.

3.2. Two bricks and mortar: micropolar point of view

Let us consider first interactions of two rigid bricks of dimensions a, b, c, connected via a thin interfacial layer of thickness $2h$, see Fig. 6. An energy stored in the layer entirely depends on the relative motion of bricks. The latter consist of relative translations and relative rotations. As in the case of rigid body dynamics, see e.g. Eremeyev et al. (2013), we can introduce the vector of translation as a displacement of their centres of mass. In addition, rotations can be described using a rotation tensor. So for two bricks we introduce two vectors of translation, i.e. $\mathbf{u}_1$ and $\mathbf{u}_2$, and two rotation tensors $\mathbf{Q}_1$ and $\mathbf{Q}_2$, respectively. As a result, the total energy of the interfacial layer can be considered as a *function* of relative translations and relative rotations

$$U_{12} = U(\mathbf{v}, \mathbf{R}), \quad \mathbf{v} = \mathbf{u}_1 - \mathbf{u}_2 = \mathbf{x}_1 - \mathbf{x}_2, \quad \mathbf{R} = \mathbf{Q}_1 \cdot \mathbf{Q}_2^T. \tag{13}$$

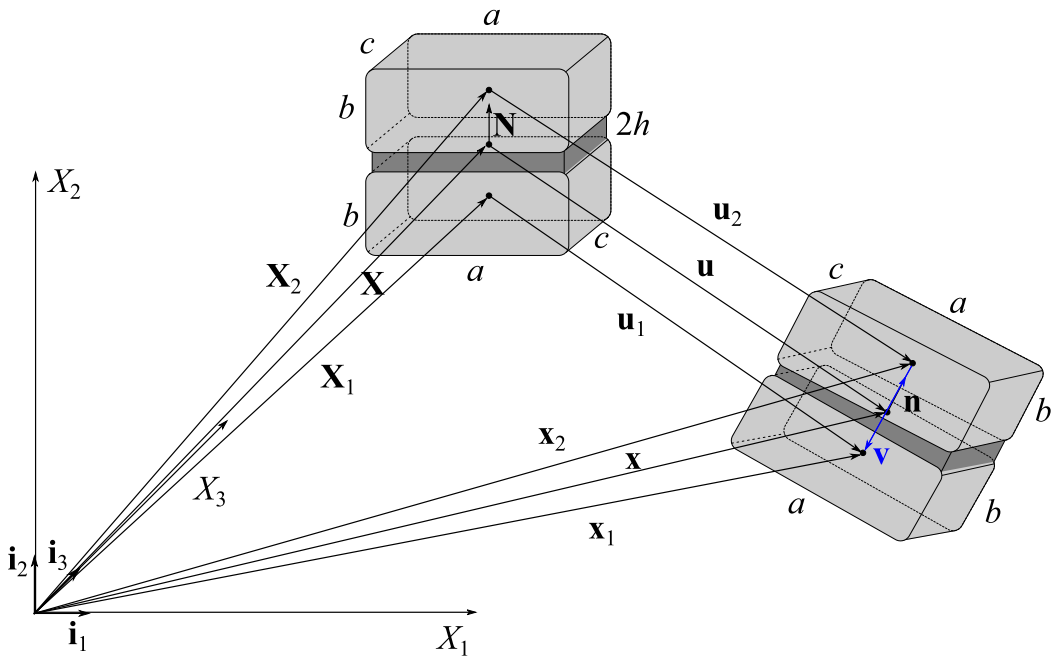

Fig. 6. Deformation of two bricks with a deformable interface.

Here $\mathbf{x}_1$ and $\mathbf{x}_2$ are the position vectors of the bricks in the current placement, see Fig. 6.

Considering our two bricks as material point of a continuum we can assume that there exist two smooth field $\mathbf{u} = \mathbf{u}(\mathbf{X}, t)$ and $\mathbf{Q} = \mathbf{Q}(\mathbf{X}, t)$ such that $\mathbf{u}_\alpha = \mathbf{u}(\mathbf{X}_\alpha, t)$ and $\mathbf{Q}_\alpha = \mathbf{Q}(\mathbf{X}_\alpha, t)$, $\alpha = 1, 2$. As a result, $\mathbf{v}$ and $\mathbf{R}$ can be represented as follows

$$\mathbf{v} \approx -2(b+h)\mathbf{F}\cdot\mathbf{N}, \quad \mathbf{R} = \mathbf{I} - 2(b+h)\mathbf{I}\times\mathbf{K}\cdot\mathbf{N}. \tag{14}$$

Here b is the thickness of the brick, $2h$ is the mean thickness of the interfacial layer, and $\mathbf{N}$ is the unit normal in the reference placement, see Fig. 6. As a result, we can see that U_{12} is a function of $\mathbf{E}$ and $\mathbf{K}$ taken at a point that is the centre of mass of the total structure, $U_{12} = U_{12}(\mathbf{E}, \mathbf{K})$. Considering the system of two bricks and the interface as a representative volume element (RVE), we can see that the deformation energy density W could be introduced as follows: $W = U_{12}/V$, where $V = 2abc + 2abh$ is total volume of the system. One can see similarities with the Cosserat point approach by Jabareen and Pestes (2020), Jabareen and Rubin (2008) and Rubin (1985, 2000). Indeed, here we replaced the 3D interfacial layer by a material point which possesses both strains as in the case of 3D Cosserat continuum.

The approach described above can be extended to a system of connected bricks. Depending on the chosen RVE we can obtain similar expression for the deformation energy density. Before we specify the form of U_{12} using three models based on experimental observations.

First, let us discuss tension-compression deformations only of two bricks as shown in Fig. 6. So here we have stretching/elongation in X_2 direction. Note that in this case $\mathbf{Q} = \mathbf{I}$ is constant. So the deformation energy stored in this system depends on E_{22} only: $W = W(E_{22})$. Considering the experimental data for tension/compression tests we can use Eq. (2) as a deformation energy.

Similarly, we can treat the shear test. From geometrical sense of $\mathbf{E}$ it follows that now W depends only on E_{12}: $W = W(E_{12})$. Again, we can use Eq. (4) as a form of W.

Taking into account the geometrical sense of $\mathbf{K}$, see Eremeyev et al. (2013) and Pietraszkiewicz and Eremeyev (2009), we can see that the stored energy related to relative rotations will have of form $W = W(K_{12})$. As a function we can use Eq. (6).

Summarizing our analysis of deformations of two bricks we can came to the following representation of the deformation energy

$$W_{12} = c_1 W_{TC}(\mathbf{i}_2\cdot\mathbf{E}\cdot\mathbf{i}_2) + c_2 W_{Sh}(\mathbf{i}_1\cdot\mathbf{E}\cdot\mathbf{i}_2) + c_3 W_B(\mathbf{i}_1\cdot\mathbf{K}\cdot\mathbf{i}_2). \tag{15}$$

Here c_1, c_2, and c_3 are normalizing coefficients related to the ratio of the volume of the mortar to the whole volume V. In the following for simplicity we assume that they are equal and we omit them just keeping the same notations for the deformation energies. Note that this equation relates to the following deformations: tension–compression in X_2 direction, shear in $X_2 - X_1$ plane, and relative rotations about X_1-axis. If we consider other shear in X_3-direction, bending about X_3-axis, and torsion about X_2-axis we came to more symmetric case

$$\begin{aligned} W_{12} =& W_{TC}(\mathbf{i}_2\cdot\mathbf{E}\cdot\mathbf{i}_2) \\ &+ W_{Sh}(\mathbf{i}_1\cdot\mathbf{E}\cdot\mathbf{i}_2) + W_{Sh}(\mathbf{i}_3\cdot\mathbf{E}\cdot\mathbf{i}_2) \\ &+ W_B(\mathbf{i}_1\cdot\mathbf{K}\cdot\mathbf{i}_2) + W_B(\mathbf{i}_3\cdot\mathbf{K}\cdot\mathbf{i}_2) + W_T(\mathbf{i}_2\cdot\mathbf{K}\cdot\mathbf{i}_2). \end{aligned} \tag{16}$$

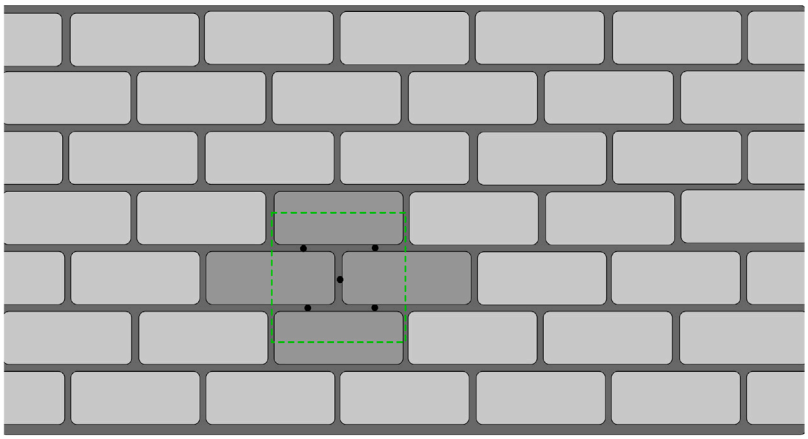

Fig. 7. Brick panel with selected RVE.

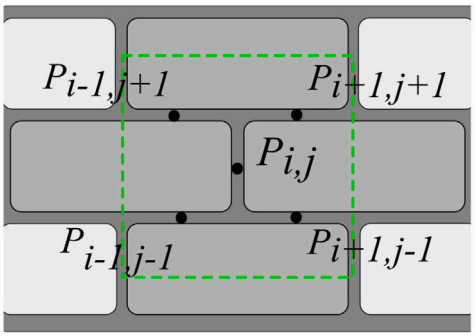

Fig. 8. RVE (bounded by dashed rectangle) with five Cosserat points.

Obviously, such a deformation energy can describe only a particular oriented material. Indeed, it has preferable direction related to X_2-axis. For a masonry consisting of a system of bricks connected in various ways this approach should be modified accordingly.

3.3. Constitutive equations of masonry-like media: micropolar point of view

Let us considering a periodic masonry, see Fig. 7, where block dimensions and joint thickness are the same reported in the previous section, see Fig. 6. The regularity of the brickwork is represented by the so-called "running bond" pattern, where each brick is surrounded by six neighbours through six interfaces. In the pattern considered, the width of the horizontal interfaces is equal to half the block width $a/2$ and the height of the vertical interfaces is equal to the block thickness b. By varying the ratio between the thickness and width b/a of the bricks, it is also possible to describe the so-called "head-bond" pattern and, more generally, to consider the influence of the local size effect due to such a periodic arrangement of bricks on the global behaviour of the masonry. In the case of periodic masonry, it is possible to identify a representative volume element (RVE) that represents the entire masonry panel through its repetition. The RVE provides all the mechanical and geometrical characteristics of the masonry at the micro level required to fully describe the entire masonry at the macro level, thus taking into account the internal microstructure. Two centre-symmetric RVEs are usually chosen for such masonry patterns (Salerno & De Felice, 2009): a classical one with a brick $B_{i,j}$ in the centre of the cell, surrounded by four horizontal and two vertical joints connecting it to the six adjacent bricks; a second one in which, instead, a vertical joint $P_{i,j}$ – modelled by means of Cosserat point, a zero-dimension Cosserat continuum – is in the centre of the cell, surrounded by four horizontal joints connecting it to four adjacent bricks. We refer to the latter RVE, reported in Fig. 8, which has been shown to be more suitable for deriving the micropolar continuum in the case of masonry, see Baraldi et al. (2015).

For the considered RVE, and referring to Eq. (16), the deformation energy is obtained by the sum of the energies W_{TC}, W_{Sh}, and W_B, related of the relative displacements and rotations ate interfaces between the four bricks:

$$\begin{aligned} W_{RVE} =& 4c_1 W_{TC}(\mathbf{i}_2 \cdot \mathbf{E} \cdot \mathbf{i}_2) + c_2 W_{TC}(\mathbf{i}_1 \cdot \mathbf{E} \cdot \mathbf{i}_1) \\ &+ 4c_1 W_{Sh}(\mathbf{i}_1 \cdot \mathbf{E} \cdot \mathbf{i}_2) + c_2 W_{Sh}(\mathbf{i}_2 \cdot \mathbf{E} \cdot \mathbf{i}_1) \\ &+ 4c_1 W_B(\mathbf{i}_1 \cdot \mathbf{K} \cdot \mathbf{i}_2) + c_2 W_B(\mathbf{i}_2 \cdot \mathbf{K} \cdot \mathbf{i}_1), \end{aligned} \tag{17}$$

where $c_1 = ah/A$, $c_2 = 2bh/A$, $A = 2ab + 2ha + 2hb$. Now the stored energy of the RVE is reduced to five Cosserat points. Considering other types of RVE one reduce the energy to another system of Cosserat points, in general. Note that the latter formula relates to in-plane deformations. It could be easily extended for 3D deformations adding additional terms.

4. Conclusions

Here we have presented a simple nonlinear model which can capture behaviour of some granular media such as a regular masonry. It is probably simplest nontrivial form of constitutive equations of micropolar solids that are relevant to observed experimental data. In particular, we assumed the additivity of energetic terms related to different types of deformations. On the other hand, such an approach is quite natural. For example, there is no coupling between compression and shear, relative rotations and shear. Nevertheless, having in hands relatively simple rheological elements one can update the model towards more complex behaviour. For example, other block-lattice structures could be considered, such as Amanat et al. (2022) and Mahoney and Siegmund (2022). Also other types of interactions could be introduced. In particular, considering long-range interactions we may come to nonlocal models that maybe essential at small scales, see e.g. recent discussions by Jiang et al. (2022), Malikan et al. (2023) and Russillo et al. (2022). Moreover, more sophisticated models of interfaces between blocks could be used here, see e.g. recent papers by Eremeyev (2024), Feng and Li (2023) and Kattis et al. (2024), and the references therein. As future developments the presented model could be used as follows. First, it could be applied for numerical analysis of deformations of masonry panels considering different masonry textures, width-to-height panel ratios and panel-to-bricks scale factors. To this end a software such as COMSOL maybe applied. In order to consider nondestructive evaluation of the masonry structures it is possible to consider ultrasonic wave propagation for different types of loading. Finally, considering nonlinearity some mathematical properties could be studied as a loss of ellipticity which can bring strain localization and further fracture of the masonry structures.

CRediT authorship contribution statement

Emanuele Reccia: Writing – review & editing, Writing – original draft, Visualization, Resources, Methodology, Investigation, Formal analysis, Conceptualization. **Victor A. Eremeyev:** Writing – review & editing, Writing – original draft, Visualization, Supervision, Investigation, Funding acquisition, Formal analysis, Conceptualization.

Declaration of competing interest

The authors declare that they have no known competing financial interests or personal relationships that could have appeared to influence the work reported in this paper.

Data availability

No data was used for the research described in the article.

Acknowledgements

This work has been supported by the project “Metamaterials design and synthesis with applications to infrastructure engineering” funded by the MUR Progetti di Ricerca di Rilevante Interesse Nazionale (PRIN) Bando 2022 - grant 20228CPHN5, Italy. V.A.E. also acknowledges the support of the European Union’s Horizon 2020 research and innovation program under the RISE MSCA EffectFact Project agreement No 101008140.

References

Addessi, D., De Bellis, M. L., & Sacco, E. (2013). Micromechanical analysis of heterogeneous materials subjected to overall Cosserat strains. *Mechanics Research Communications*, *54*, 27–34.

Addessi, D., Sacco, E., & Paolone, A. (2010). Cosserat model for periodic masonry deduced by nonlinear homogenization. *European Journal of Mechanics. A. Solids*, *29*(4), 724–737.

Amanat, S., Rafiee-Dehkharghani, R., Bitaraf, M., & Bansal, D. (2022). Analytical and numerical investigation of finite and infinite periodic lattices for mitigation of seismic waves in layered grounds. *International Journal of Engineering Science*, *173*, Article 103655.

Angelillo, M. (1993). Constitutive relations for no-tension materials. *Meccanica*, *28*, 195–202.

Anthoine, A. (1995). Derivation of the in-plane elastic characteristics of masonry through homogenization theory. *International Journal of Solids and Structures*, *32*(2), 137–163.

Bacigalupo, A., & Gambarotta, L. (2012). Computational two-scale homogenization of periodic masonry: characteristic lengths and dispersive waves. *Computer Methods in Applied Mechanics and Engineering*, *213*, 16–28.

Baraldi, D., Cecchi, A., & Tralli, A. (2015). Continuous and discrete models for masonry like material: A critical comparative study. *European Journal of Mechanics. A. Solids*, *50*, 39–58.

Baraldi, D., Reccia, E., De Carvalho Bello, C., & Cecchi, A. (2021). Laboratory and numerical experimentation for masonry in compression. *International Journal of Masonry Research and Innovation*, *6*(1), 1–20.

Capriz, G., Giovine, P., & Mariano, P. M. (Eds.), (2008). *Mathematical models of granular matter*. Berlin: Springer.

Casolo, S. (2006). Macroscopic modelling of structured materials: relationship between orthotropic Cosserat continuum and rigid elements. *International Journal of Solids and Structures*, *43*(3–4), 475–496.

Castellanos, A. (2005). The relationship between attractive interparticle forces and bulk behaviour in dry and uncharged fine powders. *Advances in Physics*, *54*(4), 263–376.
Cecchi, A., & Sab, K. (2002). A multi-parameter homogenization study for modeling elastic masonry. *European Journal of Mechanics. A. Solids*, *21*, 249–268.
Colatosti, M., Shi, F., Fantuzzi, N., & Trovalusci, P. (2023). Mechanical characterization of composite materials with rectangular microstructure and voids. *Archive of Applied Mechanics*, *93*(1), 389–404.
D'Altri, A. M., Sarhosis, V., Milani, G., Rots, J., Cattari, S., Lagomarsino, S., Sacco, E., Tralli, A., Castellazzi, G., & de Miranda, S. (2020). Modeling strategies for the computational analysis of unreinforced masonry structures: review and classification. *Acta Mechanica*, *27*, 1153–1185.
De Bellis, M. L., & Addessi, D. (2011). A Cosserat based multi-scale model for masonry structures. *International Journal for Multiscale Computational Engineering*, *9*(5).
de Gennes, P. G. (1998). Reflections on the mechanics of granular matter. *Physica A. Statistical Mechanics and its Applications*, *261*(3), 267–293.
de Gennes, P. G. (1999). Granular matter: a tentative view. *Reviews of Modern Physics*, *71*, S374–S382.
Del Piero, G. (1989). Constitutive equation and compatibility of the external loads for linear elastic masonry-like materials. *Meccanica*, *24*, 150–162.
Del Piero, G. (1998). Limit analysis and no-tension materials. *International Journal of Plasticity*, *14*(1–3), 259–271.
Dhanasekar, M., Kleeman, P. W., & Page, A. W. (1985). Biaxial stress-strain relations for brick masonry. *Journal of Structural Engineering*, *111*(5), 1085–1100.
Diana, V., Bacigalupo, A., & Gambarotta, L. (2023). Dynamic continualization of masonry-like structured materials. *Mathematics and Mechanics of Solids*, Article 10812865231205522.
Eremeyev, V. A. (2024). Surface finite viscoelasticity and surface anti-plane waves. *International Journal of Engineering Science*, *196*, Article 104029.
Eremeyev, V. A., Lebedev, L. P., & Altenbach, H. (2013). *Springer-briefs in applied sciences and technologies*, *Foundations of micropolar mechanics*. Heidelberg et al.: Springer.
Eringen, A. C. (1999). *Microcontinuum field theory I. Foundations and solids*. New York: Springer.
Feng, Y., & Li, J. (2023). A unified regularized variational cohesive fracture theory with directional energy decomposition. *International Journal of Engineering Science*, *182*, Article 103773.
Forest, S., & Sab, K. (1998). Cosserat overall modeling of heterogeneous materials. *Mechanics Research Communications*, *25*(4), 449–454.
Gatta, C., & Addessi, D. (2023). Orthotropic multisurface model with damage for macromechanical analysis of masonry structures. *European Journal of Mechanics. A. Solids*, *102*, Article 105077.
Heyman, J. (1966). The stone skeleton. *International Journal of Solids and Structures*, *2*(2), 249–279.
Hutter, K., & Rajagopal, K. R. (1994). On flows of granular materials. *Continuum Mechanics and Thermodynamics*, *6*(2), 81–139.
Jabareen, M., & Pestes, Y. (2020). The Cosserat point element as an accurate and robust finite element formulation for implicit dynamic simulations. *International Journal of Computational Methods*, *17*(01), Article 1844006.
Jabareen, M., & Rubin, M. (2008). A generalized Cosserat point element (CPE) for isotropic nonlinear elastic materials including irregular 3-D brick and thin structures. *Journal of Mechanics of Materials and Structures*, *3*(8), 1465–1498.
Jiang, Y., Li, L., & Hu, Y. (2022). A nonlocal surface theory for surface–bulk interactions and its application to mechanics of nanobeams. *International Journal of Engineering Science*, *172*, Article 103624.
Kachanov, M., & Sevostianov, I. (2005). On quantitative characterization of microstructures and effective properties. *International Journal of Solids and Structures*, *42*(2), 309–336.
Kattis, M., Tsitsos, V., & Karatzaferis, V. (2024). Weakened interfaces in Cosserat bi-materials with constrained rotation. *International Journal of Engineering Science*, *194*, Article 103970.
Lemos, J. V. (2007). Discrete element modeling of masonry structures. *International Journal of Architectural Heritage*, *1*, 190–213.
Lourenço, P. B. (2010). Recent advances in masonry modelling: micromodelling and homogenisation. *Multiscale Modeling in Solid Mechanics: Computational Approaches*, 251–294.
Lourenço, P. B., Milani, G., Tralli, A., & Zucchini, A. (1997). Analysis of masonry structures: Review of and recent trends in homogenization techniques. *Canadian Journal of Civil Engineering*, *34*, 1443–1457.
Lourenço, P. B., Rots, J. G., & Blaauwendraad, J. (1998). Continuum model for masonry: parameter estimation and validation. *Journal of Structural Engineering*, *124*(6), 642–652.
Luciano, R., & Sacco, E. (1997). Homogenization technique and damage model for old masonry material. *International Journal of Solids and Structures*, *34*(24), 3191–3208.
Magenes, G., & Calvi, G. M. (1997). In-plane seismic response of brick masonry walls. *Earthquake Engineering & Structural Dynamics*, *26*, 1091–1112.
Mahoney, K., & Siegmund, T. (2022). Mechanics of tubes composed of interlocking building blocks. *International Journal of Engineering Science*, *174*, Article 103654.
Malikan, M., Dastjerdi, S., Eremeyev, V. A., & Sedighi, H. M. (2023). On a 3D material modelling of smart nanocomposite structures. *International Journal of Engineering Science*, *193*, Article 103966.
Masiani, R., Rizzi, N., & Trovalusci, P. (1995). Masonry as structured continuum. *Meccanica*, *30*, 673–683.
Masiani, R., & Trovalusci, P. (1996). Cosserat and Cauchy materials as continuum models of brick masonry. *Meccanica*, *31*, 421–432.
Nedderman, R. M. (1992). *Statics and kinematics of granular materials*. Cambridge: Cambridge University Press.
Page, A. W. (1981). The biaxial compressive strength of brick masonry. *Proceedings of the Institution of Civil Engineers*, *71*(3), 893–906.
Pau, A., & Trovalusci, P. (2012). Block masonry as equivalent micropolar continua: the role of relative rotations. *Acta Mechanica*, *223*(7), 1455–1471.
Pietraszkiewicz, W., & Eremeyev, V. A. (2009). On natural strain measures of the non-linear micropolar continuum. *International Journal of Solids and Structures*, *46*(3–4), 774–787.
Rajagopal, K. R. (2011). Non-linear elastic bodies exhibiting limiting small strain. *Mathematics and Mechanics of Solids*, *16*(1), 122–139.
Reccia, E., Leonetti, L., Trovalusci, P., & Cecchi, A. (2018). A multiscale/multidomain model for the failure analysis of masonry walls: A validation with a combined FEM/DEM approach. *International Journal for Multiscale Computational Engineering*, *16*(4), 325–343.
Rubin, M. B. (1985). On the theory of a Cosserat point and its application to the numerical solution of continuum problems. *Journal of Applied Mechanics*, *52*(2), 368–372.
Rubin, M. B. (2000). *Solid mechanics and its applications*: *vol. 79*, *Cosserat theories: shells, rods and points*. Dordrecht: Kluwer.
Russillo, A. F., Failla, G., Barretta, R., & de Sciarra, F. M. (2022). On the dynamics of 3D nonlocal solids. *International Journal of Engineering Science*, *180*, Article 103742.
Sacco, E. (2009). A nonlinear homogenization procedure for periodic masonry. *European Journal of Mechanics. A. Solids*, *28*(2), 209–222.
Salerno, G., & De Felice, G. (2009). Continuum modeling of periodic brickwork. *International Journal of Solids and Structures*, *46*(5), 1251–1267.
Stefanou, I., Sulem, J., & Vardoulakis, I. (2008). Three-dimensional Cosserat homogenization of masonry structures: elasticity. *Acta Geotechnica*, *3*, 71–83.
Suiker, A. S. J., & de Borst, R. (2005). Enhanced continua and discrete lattices for modelling granular assemblies. *Philosophical Transactions of the Royal Society A*, *363*(1836), 2543–2580.
Tejchman, J. (2008). *Shear localization in granular bodies with micro-polar hypoplasticity*. Berlin: Springer.
Thatikonda, N., Baraldi, D., Boscato, G., & Cecchi, A. (2024). Experimental evaluation of elastic shear components for masonry in a Cosserat continuum. *International Journal of Solids and Structures*, *292*, Article 112715.

Tian, J., Lai, Y., Liu, E., & He, C. (2023). A thermodynamics-based micro-macro elastoplastic micropolar continuum model for granular materials. *Computers and Geotechnics*, *162*, Article 105653.

Trovalusci, P., & Masiani, R. (2003). Non-linear micropolar and classical continua for anisotropic discontinuous materials. *International Journal of Solids and Structures*, *40*(5), 1281–1297.

Trovalusci, P., & Pau, A. (2014). Derivation of microstructured continua from lattice systems via principle of virtual works: the case of masonry-like materials as micropolar, second gradient and classical continua. *Acta Mechanica*, *225*(1), 157–177.

Vasconcelos, G., & Lourenço, P. B. (2009a). Experimental characterization of stone masonry in shear and compression. *Construction and Building Materials*, *23*(11), 3337–3345.

Vasconcelos, G., & Lourenço, P. B. (2009b). In-plane experimental behavior of stone masonry walls under cyclic loading. *Journal of Structural Engineering*, *135*(10), 1269–1277.